



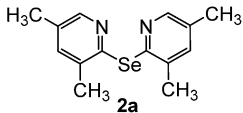
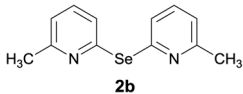
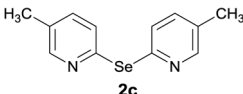
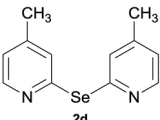
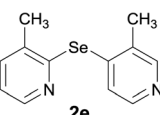
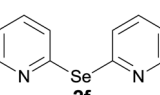
CrossMark
← click for updates

Results and discussion

Bis(3,5-dimethyl-2-pyridyl)diselenide (**1a**) was reacted with LiAlH_4 in THF at 10°C . The reaction mixture was slowly brought to the room temperature and refluxed for 16 h. The progress of the reaction was monitored by TLC and GC-MS analysis. The reaction was stopped when all of the diselenide was completely consumed. After the work-up and purification procedures, bis(3,5-dimethyl-2-pyridyl)selenide (**2a**) was obtained in an excellent yield (entry 1, Table 1). Following the same procedure, other bis(2-pyridyl)selenides (**2b–2f**) were also synthesized (entries 2–6, Table 1).

In order to check the influence of the solvent on the rate of the reaction, these reactions were also carried out in DMF. Contrary to the expectation, the reactions in DMF were almost two times slower than in THF. In addition, the yields of the reactions were lower than in THF (Table 1). The comparative lower yields in DMF could be due to the competing reaction of LiAlH_4 with DMF. LiAlH_4 has the tendency to react with alkyl/arylamides to give the corresponding amines.

Table 1 Synthesis of bis(2-pyridyl)selenides by using LiAlH_4

Sr. no.	DS	Time (h)		Product	Yield (%)	
		THF	DMF		THF	DMF
1	1a	16	36		95	89
2	1b	17	36		92	89
3	1c	15	40		90	86
4	1d	17	40		91	84
5	1e	15	40		90	83
6	1f	16	46		96	88

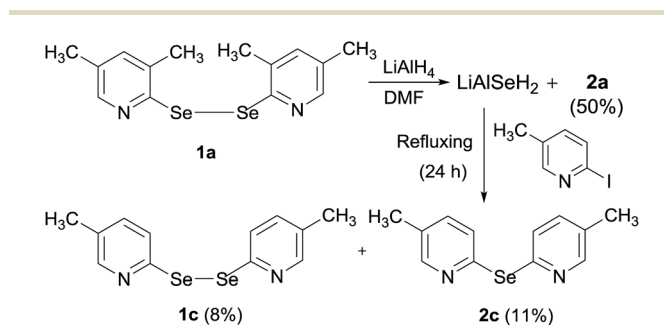
Mechanistic study

The exclusive formation of monoselenides suggests that one of the two $\text{C}_{(\text{pyridine})}\text{--Se}$ bonds in bis(2-pyridyl)diselenides is selectively cleaved in the presence of LiAlH_4 . This is contrary to the generally accepted exposition that the treatment of a reducing agent, such as LiAlH_4 ,¹² NaBH_4 ,⁴ $\text{Li}(\text{C}_2\text{H}_5)_3\text{BH}$,¹⁶ *etc.*, with bis(organyl)diselenide cleaves the Se–Se bond and generate the corresponding organylselenenols/selenolates only. It is pertinent to mention that there is no report that mentions the scission of the C–Se bond in bis(organyl)diselenide.

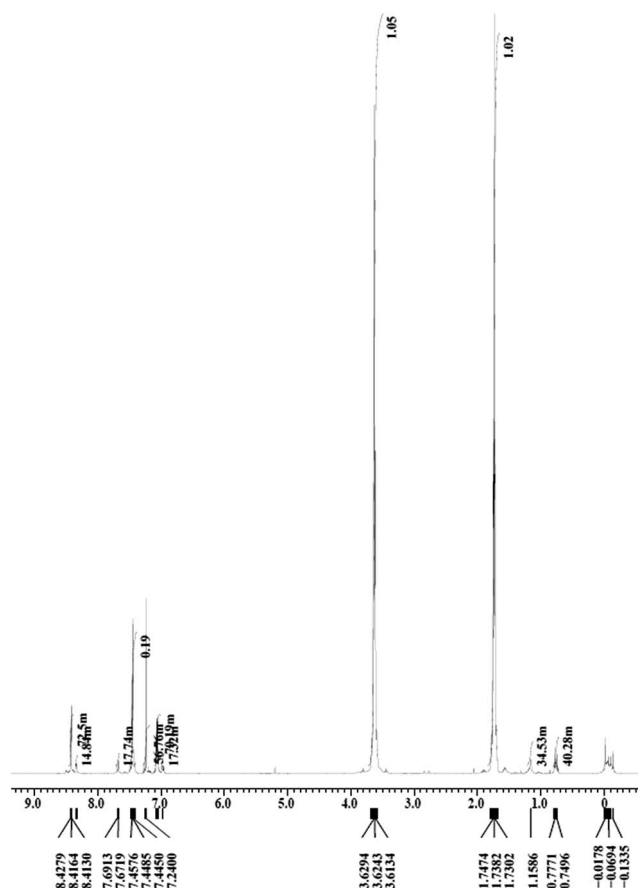
It is further postulated that LiAlH_4 retains the cleaved selenium atom resulting in the formation of LiAlSeH_2 . To confirm the formation of LiAlSeH_2 , we added 2-iodo-5-methylpyridine to a mixture of (**1a**) and LiAlH_4 . Our thinking was that 2-iodo-5-methylpyridine would react with the *in situ* formed LiAlSeH_2 and afford the corresponding mono- or diselenide. This was actually the case as bis(5-methyl-2-pyridyl)diselenide (**1c**) and bis(5-methyl-2-pyridyl)selenide (**2c**) along with **2a** were obtained from the reaction mixture (Scheme 1). The lower yield of the products is mainly due to the difficulty in the purification of the crude product by column chromatography. Since these products travelled very closely in the chromatographic column, the chromatography procedure was performed three times to get analytically pure products.

The generation of LiAlSeH_2 was also confirmed by the NMR analysis. A mixture of (**1c**) and LiAlH_4 was refluxed in THF for 15 h. The solvent from the reaction mixture was removed and a solid greyish powder was obtained. The ^1H NMR spectrum of the powder was taken in CDCl_3 that showed two prominent peaks at δ 1.74 and 3.62 ppm (Fig. 1). These chemical shift values are close to those reported by Ishihara *et al.* for LiAlSeH_2 .¹¹ The latter two observations confirms the formation of LiAlSeH_2 during the reaction of LiAlH_4 with bis(2-pyridyl)diselenides.

From the aforementioned facts, the following mechanistic steps have been proposed. The first step is a fast reaction involving the cleavage of the Se–Se bond and simultaneous formation of a selenated aluminato complex (**I**) (Scheme 2). Lithium is attached to the one of two pyridine rings (from the optimized structure, Fig. 2, discussed later) and this ring behaves as an electrophile and initiates the reaction involved in the second step. The second step is a slow and energy intensive process that involves the transfer of one of the two pyridyl moieties, attached to the complex **I**, to the adjacent pySe unit as

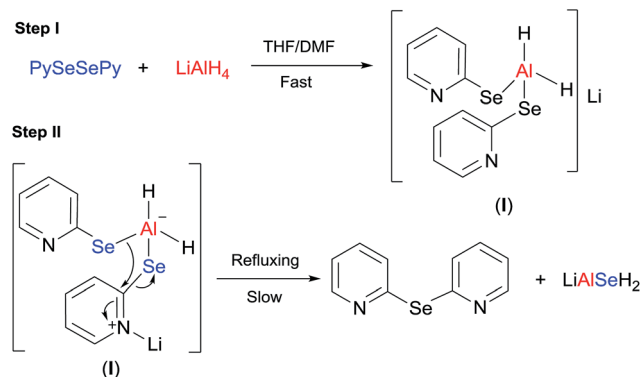


Scheme 1 Reaction sequence exhibiting the generation of LiAlSeH_2 .



shown in Scheme 2 (pyridine-shift reaction). This generates bis(2-pyridyl)selenide and LiAlSeH_2 as the final products.

The mechanism was tested by investigating a number of reactions. Bis(2-pyridyl)diselenide was refluxed in DMF/THF for

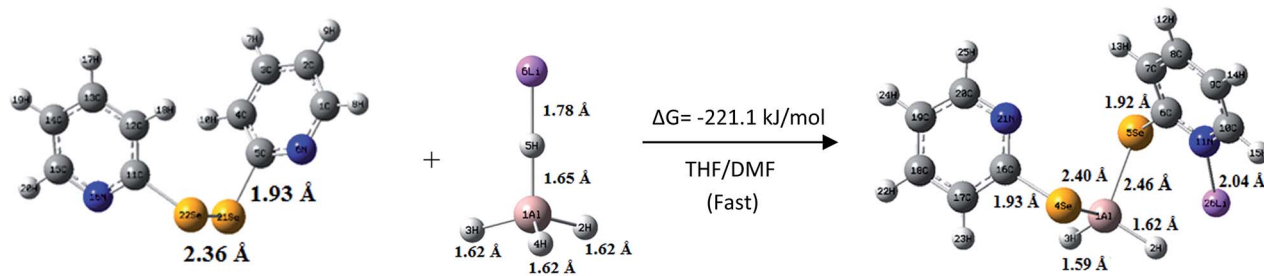


Scheme 2 Mechanism of the reaction.

48 h but there was no indication of the formation of the corresponding monoselenide. This indicates that the diselenide is perfectly stable at elevated temperatures and it is LiAlH_4 that aids in the formation of the monoselenide. Further, the reaction of LiAlH_4 and bis(2-pyridyl)selenide in DMF and THF was investigated. In spite of refluxing the reaction mixture for more than 48 h, no interaction between LiAlH_4 and bis(2-pyridyl)selenide was observed. This establishes that the cleavage of Se–Se bond with LiAlH_4 precedes the formation of the aluminate complex (**I**) and subsequently the pyridine-shift reaction. In another variation, we examined the reaction of bis(2-pyridyl)diselenide with NaBH_4 in DMF. The solution containing the diselenide and NaBH_4 was refluxed for several hours; however there was no indication of the formation of the monoselenide. All these observations suggests an unique ability of LiAlH_4 in inducing the cleavage of C–Se bond in bis(2-pyridyl)diselenides.

In our earlier studies,¹² we have reported the synthesis of unsymmetrical selenides from the reaction of diselenides with LiAlH_4 followed by treatment with a strong electrophile such as

Step I: Formation of selenated aluminato complex (I)



Step II: Pyridine-shift reaction

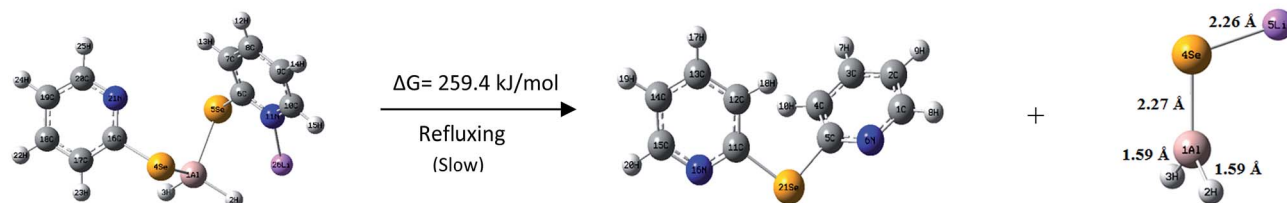


Fig. 2 Reaction mechanism with optimized structures of reactants, products and intermediate species.

iodomethane. We revisited this chemistry in order to investigate if any symmetrical monoselenide is formed in this reaction also. Bis(2-pyridyl)diselenide was reacted with LiAlH_4 in THF at -10°C . The resulting reaction mixture was treated with iodomethane and refluxed for 36 h. During this time the reaction was continuously monitored by GC-MS. There was no trace of bis(2-pyridyl)selenide at any time of the reaction. The whole of bis(2-pyridyl)diselenide was converted into (2-methylselenenyl)pyridine (Scheme 3). It appears that the attack of CH_3I on the complex, **I**, is faster and more favourable than the pyridine-shift reaction.

Theoretical validation of the mechanism

Gibbs free energy was calculated by using the closed-shell Becke–Lee–Yang–Parr hybrid exchange–correlation three-parameter functional (B3LYP) in combination with 6-31 + G(d,p) basis set in THF solvent to theoretically support the reaction mechanism shown in Scheme 2. The reaction shown in step I involves Gibbs free energy change (ΔG) of 221.1 kJ mol^{-1} which strongly provides evidence of a spontaneous reaction involving the formation of the aluminato complex (**I**) (Fig. 2). The second step involves a positive ΔG value of 259.4 kJ mol^{-1} , which indicates an energy intensive process. This actually is the case as the second step requires refluxing for a long duration of time. The optimized structures of **1f**, LiAlH_4 , aluminato complex and LiAlSeH_2 are given in Fig. 2. The optimized structures of **1f** and LiAlH_4 agree well with the corresponding experimentally determined structures.^{6,17} The Al–H bond distances are shorter in LiAlSeH_2 than in LiAlH_4 . Lithium is attached to the Se atom in LiAlSeH_2 , whereas it is bonded to one of the four hydrogen atoms in LiAlH_4 .

Synthesis of monoselenides directly from elemental selenium and LiAlH_4

Next, we investigated the direct formation of monoselenides from the reaction of LiAlH_4 and elemental selenium. LiAlH_4 (1.0

equiv.) was added to a suspension of elemental selenium in dry DMF. A grayish suspension indicating the formation of LiAlSeH_2 was obtained. Addition of 2-bromopyridine (1.0 equiv.) to this suspension and 3 h refluxing gave bis(2-pyridyl)selenide (**2f**) and bis(2-pyridyl)diselenide (**1f**) in 72% and 23% yields, respectively (Scheme 4).

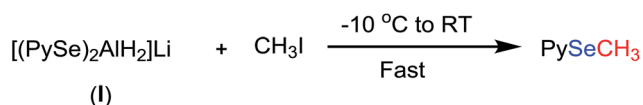
Following the same procedure, other bis(2-pyridyl)selenides (**2b–2e**) and bis(2-pyridyl)diselenides (**1b–1e**) were also obtained (Scheme 4 and Table 2). Interestingly, in all these reactions the monoselenide was the major product formed even when the proportion of 2-bromopyridine was increased from 1.0 equiv. to 2.0 equiv. With the other reported methodologies,^{5a,12,18} the diselenide is always the major product formed. It appears that this methodology is more suitable for the synthesis of bis(2-pyridyl)selenides instead of bis(2-pyridyl)diselenides. Part of this appears to come from the scission of C–Se bond in bis(2-pyridyl)diselenide.

Single crystal X-ray structure determination of **2e**

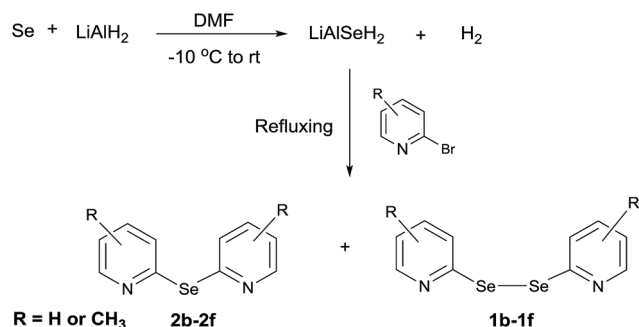
The crystals of **2e** suitable for X-ray diffraction analysis were grown by a slow evaporation of a saturated solution of hexane and ethyl acetate. A thermal ellipsoid drawing of **2e**, presented in Fig. 3, shows that the molecule adopts a twisted conformation, in which the nitrogen atoms of two pyridine rings face each other with a dihedral angle between the two aromatic rings of $66.69(7)^\circ$. The selected bond lengths involving the selenium centre, gathered in Table 3, are in close agreement with those

Table 2 Synthesis of mono- and diselenides of pyridine

Entry	Starting material	Products	
		Monoselenide	Diselenide
1	2 Bromo 6 methylpyridine	2b (69%)	1b (24%)
2	2 Bromo 5 methylpyridine	2c (71%)	1c (22%)
3	2 Bromo 4 methylpyridine	2d (70%)	1d (27%)
4	2 Bromo 3 methylpyridine	2e (70%)	1e (26%)
5	2 Bromopyridine	2f (72%)	1f (23%)



Scheme 3 Reaction of aluminato complex (**I**) with iodomethane.



Scheme 4 Synthesis of bis(2-pyridyl)selenides and -diselenides.

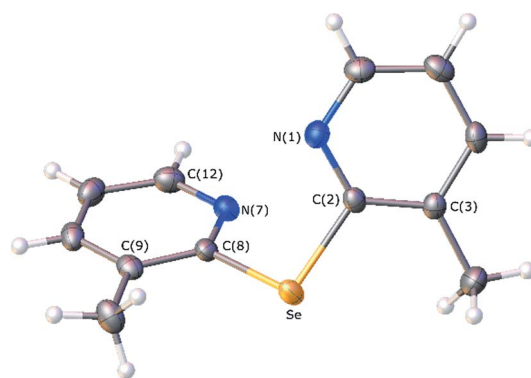


Fig. 3 Molecular structure of bis(3-methyl-2-pyridyl)selenide (**2e**) with thermal ellipsoids drawn at the 50% probability level. Selenium, nitrogen, carbon and hydrogen atoms are drawn in orange, light blue, grey and white, respectively.

Table 3 Selected bond distances (Å) and angles (°) of **2e**

Se C(2)	1.934(2)	Se C(8)	1.933(2)
C(2) Se C(8)	97.90(8)		
Se C(2) C(3)	119.46(15)	Se C(8) C(9)	119.43(15)
Se C(2) N(1)	115.61(15)	Se C(8) N(7)	115.87(15)

determined for bis(2-pyridyl)selenide analogue **2f**.¹⁹ However, in this compound a different conformation is adopted, which is characterized by the opposite spatial disposition of the pyridine nitrogen relatively to the C–Se–C central fragment and a dihedral angle of 52.5° between pyridine rings.

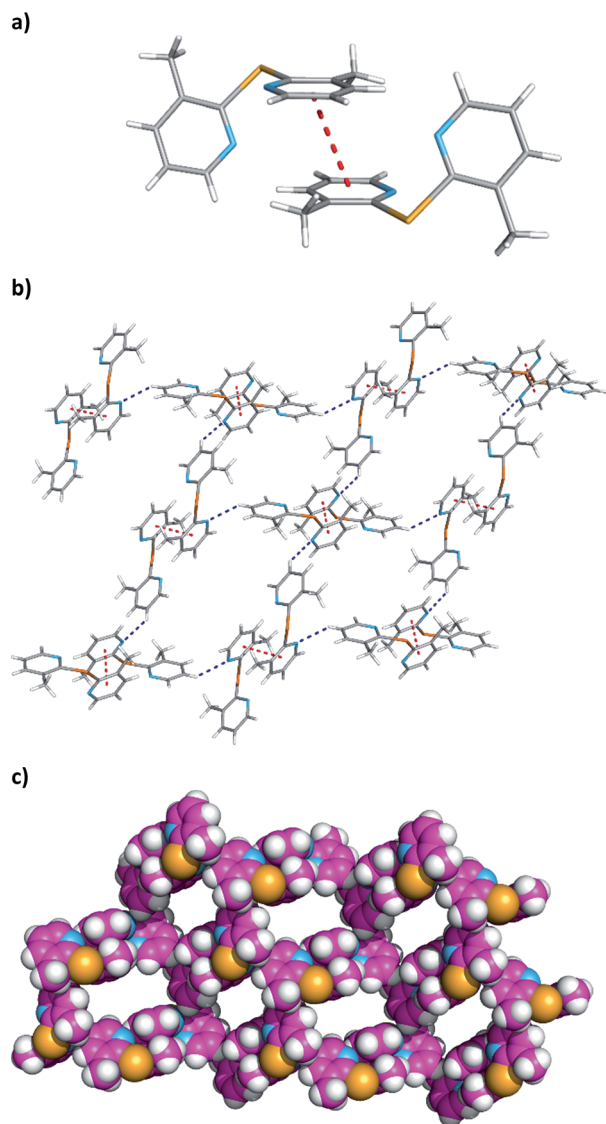


Fig. 4 Crystal packing diagram features of **2e**: view (a) shows the formation of a dimer via $\pi\cdots\pi$ interactions; view (b) shows a 2-D network built up through the self-assembly of $\pi\cdots\pi$ dimer units by subsequent H \cdots N hydrogen bonds (c) CPK representation of 2-D network emphasising the empty regions determined by ring motifs composed of four adjacent dimers. Colour scheme as described in Fig. 3, apart the carbon atoms in view (c), which are in light magenta. The $\pi\cdots\pi$ interactions between the pyridine rings and hydrogen bonds are drawn as red and dark blue dashed lines, respectively.

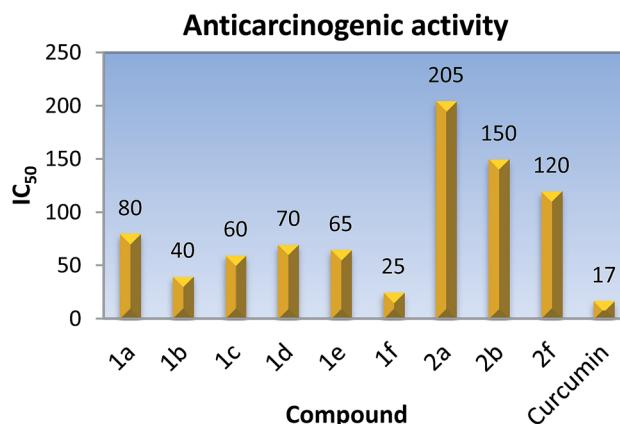


Fig. 5 IC₅₀ values of bis(2-pyridyl)selenides and -diselenides against the Raji cancer cell line.

The relevant crystal packing features of **2e** are depicted in Fig. 4. In the crystal lattice, two adjacent molecules are stacked over one another with a centroid–centroid distance of 3.612(2) Å and a shift distance of 1.391(3) Å. These distances are consistent with the existence of $\pi\cdots\pi$ stacking interactions resulting in the formation of a dimer as shown in Fig. 4a. The dimers are further self-assembled through C–H \cdots N hydrogen bonds with C \cdots N distances of 3.413(3) Å and C–H \cdots N angles of 142°. Thus, the crystal structure exists as a 2-D network of $\pi\cdots\pi$ interactions and C–H \cdots N hydrogen bonds. This network grows up from a ring motif composed of four dimer entities as illustrated in Fig. 4b and c.

Anticarcinogenic activity

Anticarcinogenic activity of the synthesized compounds was screened at different concentrations against the Raji cancer cell line, (acute lymphoid leukemia) cells using the MTT colorimetric assay.²⁰ The MTT assay is based on the reduction of the yellow soluble 3-(4,5-methyl-2-thiazolyl)-2,5-diphenyl-2H-tetrazolium bromide (MTT) into a blue-purple formazan product, mainly by mitochondrial succinic dehydrogenase enzyme activity inside living cells. Curcumin is a known anticancer compound which has been considered as a positive control in the present study. The results were expressed as the IC₅₀, inducing a 50% inhibition of cell growth of treated cells when compared to the growth of control cells. **1f** showed the maximum activity and possessed IC₅₀ at 25 μM. A perusal of the data in Fig. 5 reveals that the anticarcinogenic activity of the pyridylseleniums decreases with the increase in the number of methyl groups (Fig. 5). Further, it was found that the bis(2-pyridyl)diselenides are 2–5 times more active than the corresponding monoselenides, Fig. 5. The standard drug curcumin shows IC₅₀ at about 17 μM against the Raji cancer cell line and the activity of the compound **1f** is very close to it.

Experimental

All the experiments were carried out in a dry oxygen-free nitrogen atmosphere and the solvents were dried before use.

^1H and ^{13}C NMR spectra were recorded on a Bruker 400 MHz spectrophotometer in CDCl_3 . The EI mass spectra were taken by using Shimadzu GC-Mass Spectrometer [GCMS QP-2010 plus] with Rtx-1MS (30 m \times 0.25 mm ID \times 0.25 μm) capillary column. The elemental analysis was carried out by using Elementar Vario MICRO analyser.

General procedure: preparation of bis(2-pyridyl)selenides

LiAlH_4 (0.06 g, 1.70 mmol) was added in small installments to a vigorously stirred solution of bis(2-pyridyl)diselenide (1.30 mmol) in dry THF or DMF at 10°C . The grayish yellow suspension was slowly warmed to room temperature and then refluxed for 12–46 h in an oil-bath. The formation of mono-selenide was monitored by TLC and GC-MS. After completion, the reaction mixture was hydrolyzed with 30 mL of distilled water. The organic layer was extracted with diethyl ether (3 \times 50 mL), washed with water, and then dried over anhydrous sodium sulfate. The solvent was removed and the crude product was purified by column chromatography using 60–120 mesh silica gel and hexane–ethyl acetate as an eluent (20 : 1).

Bis(3,5-dimethyl-2-pyridyl)selenide (2a). Diselenide:- bis(3,5-dimethyl-2-pyridyl)diselenide (0.46 g, 1.30 mmol). Yield: 0.35 g 95% (THF), 0.32 g 89% (DMF), m.p. $125\text{--}127^\circ\text{C}$. ^1H NMR: CDCl_3 , 400 MHz δ (ppm): 8.14 (s, 2H), 7.18 (s, 2H), 2.41 (s, 6H), 2.24 (s, 6H). ^{13}C NMR: CDCl_3 , 400 MHz δ (ppm): 149.9, 148.2, 137.9, 133.8, 131.8, 20.8, 17.7. MS (EI, 70 eV) m/z (relative intensity): 292 (18), 197 (52), 106 (22), 91 (100), 77 (24), 65 (49). Anal. calcd (%) for $\text{C}_{14}\text{H}_{16}\text{N}_2\text{Se}$: C, 57.73, H, 5.53, N, 9.61. Found: C, 57.82, H, 5.51, N, 9.60.

Bis(6-methyl-2-pyridyl)selenide (2b). Diselenide:- bis(6-methyl-2-pyridyl)diselenide (0.44 g, 1.30 mmol). Yield: 0.32 g 92% (THF), 0.31 g 89% (DMF), m.p. $120\text{--}122^\circ\text{C}$. ^1H NMR: CDCl_3 , 400 MHz δ (ppm): 7.42 (t, 2H), 7.30–7.32 (d, $J = 7.7$ Hz, 2H), 6.99–7.01 (d, $J = 7.4$ Hz, 2H), 2.54 (s, 6H). ^{13}C NMR: CDCl_3 , 400 MHz δ (ppm): 159.3, 154.4, 137.0, 124.8, 121.4, 24.3. MS (EI, 70 eV) m/z (relative intensity): 264 (100), 222 (1), 183 (48), 168 (16), 131 (6), 92 (66), 65 (100), 51 (44). Anal. calcd (%) for $\text{C}_{12}\text{H}_{12}\text{N}_2\text{Se}$: C, 54.76, H, 4.59, N, 10.64. Found: C, 54.59, H, 4.55, N, 10.67.

Bis(5-methyl-2-pyridyl)selenide (2c). Diselenide:- bis(5-methyl-2-pyridyl)diselenide (0.44 g, 1.30 mmol). Yield: 0.31 g 90% (THF), 0.30 g 86% (DMF), m.p. $94\text{--}95^\circ\text{C}$. ^1H NMR: CDCl_3 , 400 MHz δ (ppm): 8.28–8.28 (d, $J = 1.9$ Hz, 2H), 7.67–7.69 (d, $J = 8.1$ Hz, 2H), 7.33–7.36 (d, $J = 2.2$, 8.1 Hz, 2H), 2.28 (s, 3H). ^{13}C NMR: CDCl_3 , 400 MHz δ (ppm): 150.9, 149.8, 138.2, 130.9, 123.4, 17.8. MS (ESI) m/z (relative intensity): 263 (76), 247 (1), 183 (6), 168 (3), 93 (39), 65 (100), 53 (5). Anal. calcd (%) for $\text{C}_{12}\text{H}_{12}\text{N}_2\text{Se}$: C, 54.76, H, 4.59, N, 10.64. Found: C, 55.64, H, 4.53, N, 10.61.

Bis(4-methyl-2-pyridyl)selenide (2d). Diselenide:- bis(4-methyl-2-pyridyl)diselenide (0.44 g, 1.30 mmol). Yield: 0.31 g 91% (THF), 0.29 g 84% (DMF), m.p. $130\text{--}132^\circ\text{C}$. ^1H NMR: CDCl_3 , 400 MHz δ (ppm): 8.29–8.31 (d, $J = 5.0$ Hz, 2H), 7.61 (s, 2H), 6.88–6.89 (d, $J = 5.1$ Hz, 2H), 2.28 (s, 6H). ^{13}C NMR: CDCl_3 , 400 MHz δ (ppm): 154.2, 149.1, 123.9, 122.4, 96.1, 21.1. MS (EI, 70 eV) m/z (relative intensity): 264 (39), 243 (89), 249 (73), 183 (13), 168 (14), 132 (57), 92 (33), 65 (100), 51 (64). Anal. calcd (%) for $\text{C}_{12}\text{H}_{12}\text{N}_2\text{Se}$: C, 54.76, H, 4.59, N, 10.64. Found: C, 54.73, H, 4.53, N, 10.69.

Bis(3-methyl-2-pyridyl)selenide (2e). Diselenide:- bis(3-methyl-2-pyridyl)diselenide (0.44 g, 1.30 mmol). Yield: 0.30 g 90% (THF), 0.29 g 83% (DMF), m.p. $177\text{--}182^\circ\text{C}$. ^1H NMR: (CDCl_3 , 400 MHz): δ (ppm): 8.47–8.49 (dd, $J = 1.9$, 4.7 Hz, 2H), 7.38–7.41 (dd, $J = 4.7$, 7.5 Hz, 2H), 6.87 (t, 2H), 2.19 (s, 6H). ^{13}C NMR: (CDCl_3 , 400 MHz): δ (ppm): 140.3, 138.4, 132.7, 125.0, 120.3, 25.7. MS (EI, 70 eV) m/z (relative intensity): 266 (8), 264 (41), 249 (65), 183 (100), 172 (6), 168 (40), 51 (9). Anal. calcd (%) for $\text{C}_{12}\text{H}_{12}\text{N}_2\text{Se}$: C, 54.76, H, 4.59, N, 10.64. Found: C, 54.88, H, 4.51, N, 10.60.

Bis(2-pyridyl)selenide (2f).^{4c} Diselenide:- bis(2-pyridyl)diselenide (0.40 g, 1.30 mmol). Yield: 0.29 g 96% (THF), 0.27 g 88% (DMF), m.p. $93\text{--}94^\circ\text{C}$. ^1H NMR: CDCl_3 , 400 MHz δ (ppm): 8.53–8.54 (ddd, $J = 1.5$, 2.6, 4.8 Hz, 2H), 7.54–7.59 (m, 2H), 7.14–7.19 (m, 2H). ^{13}C NMR: CDCl_3 , 400 MHz δ (ppm): 155.0, 150.4, 137.0, 128.1, 121.9. MS (EI, 70 eV) m/z (relative intensity): 235 (42), 155 (7), 78 (98), 51 (100). Anal. calcd (%) for $\text{C}_{10}\text{H}_8\text{N}_2\text{Se}$: C, 51.07, H, 3.42, N, 8.01. Found: C, 51.12, H, 3.48, N, 7.97.

Synthesis of selenides from elemental selenium and LiAlH_4

Selenium (1 g, 12.66 mmol) powder and dry DMF were taken in a three necked 100 mL RBF. The temperature of the reaction mixture was lowered to 10°C and LiAlH_4 (0.48 g, 12.66 mmol) was added in small instalments under dry oxygen free nitrogen atmosphere. The grayish suspension was formed and slowly brought to the room temperature. The reaction mixture was stirred at room temperature for 30 min and again re-cooled to 0°C and then 2-bromopyridine (12.66 mmol) was added to it in a drop-wise manner. The reaction mixture was slowly brought to the room temperature and then, refluxed for 3 h at 140°C . The process of reaction was monitored by TLC. After the completion of reaction, the solvent was removed under vacuum with the help of a rota-evaporated. The solid residue was dissolved in chloroform (50 mL) and the organic layer was washed with water. The organic layer was then dried over anhydrous sodium sulfate. The solvent was removed and the crude product was purified by column chromatography using 60–120 mesh silica gel and hexane–ethyl acetate as an eluent. Following the same procedure, other bis(2-pyridyl)selenides and bis(2-pyridyl)diselenides were also prepared.

Bis(6-methyl-2-pyridyl)diselenide (1b).^{5a} M.p. $61\text{--}62^\circ\text{C}$. ^1H NMR: (CDCl_3 , 400 MHz): δ (ppm): 7.53–7.55 (d, $J = 8.3$ Hz, 2H), 7.39–7.41 (d, $J = 8.3$ Hz, 1H), 2.55 (s, 3H). ^{13}C NMR: (CDCl_3 , 400 MHz): δ (ppm): 150.8, 149.8, 138.2, 130.9, 123.4, 17.8. MS (ESI): 344 (^{80}Se). Anal. calcd (%) for $\text{C}_{12}\text{H}_{12}\text{N}_2\text{Se}_2$: C, 42.12, H, 3.53, N, 8.18. Found: C, 41.85, H, 3.59, N, 8.08.

Bis(5-methyl-2-pyridyl)diselenide (1c).^{5a} M.p. $65\text{--}66^\circ\text{C}$. ^1H NMR: CDCl_3 , 400 MHz δ (ppm): 8.28 (s, 2H), 7.68–7.70 (d, $J = 8.1$ Hz, 2H), 7.34–7.36 (dd, $J = 1.9$, 8.1 Hz, 2H), 2.29 (s, 6H). ^{13}C NMR: (CDCl_3 , 400 MHz): δ (ppm): 150.8, 149.8, 138.2, 130.9, 123.4, 17.8. MS (ESI): 344 (^{80}Se). Anal. calcd (%) for $\text{C}_{12}\text{H}_{12}\text{N}_2\text{Se}_2$: C, 42.12, H, 3.53, N, 8.18. Found: C, 41.87, H, 3.56, N, 8.10.

Bis(4-methyl-2-pyridyl)diselenide (1d).^{5a} M.p. $96\text{--}98^\circ\text{C}$. ^1H NMR: (CDCl_3 , 400 MHz): δ (ppm): 8.31–8.29 (d, $J = 4.9$ Hz, 2H), 7.65 (s, 2H), 6.90–6.91 (d, $J = 4.1$ Hz, 2H), 2.29 (s, 6H). ^{13}C NMR: (CDCl_3 , 400 MHz): δ (ppm): 154.1, 149.1, 148.9, 123.9, 122.4,

21.0. MS (EI, 70 eV) m/z (relative intensity): 344 (10), 263 (5), 183 (59), 92 (99), 80 (6), 65 (100), 51 (7). Anal. calcd (%) for $C_{12}H_{12}N_2Se_2$: C, 42.12, H, 3.53, N, 8.18. Found: C, 42.21, H, 3.40, N, 8.03.

Bis(3-methyl-2-pyridyl)diselenide (1e).^{5a} M.p. 142–144 °C. 1H NMR: ($CDCl_3$, 400 MHz): δ (ppm): 8.28–8.30 (d, $J = 5.9$ Hz, 2H), 7.26–7.34 (d, $J = 7.4$ Hz, 2H), 7.00–7.03 (t, $J = 7.4$ Hz, 2H), 2.46 (s, 6H). ^{13}C NMR: ($CDCl_3$, 400 MHz): δ (ppm): 153.3, 147.9, 136.8, 133.7, 121.8, 20.7. MS (EI, 70 eV) m/z (relative intensity): 264 (42), 249 (65), 183 (100), 168 (40), 131 (8), 92 (29), 65 (4), 51 (9). Anal. calcd (%) for $C_{12}H_{12}N_2Se_2$: C, 54.76, H, 4.59, N, 10.64. Found: C, 54.86, H, 4.51, N, 10.76.

Bis(2-pyridyl)diselenide (1f).²¹ M.p. 48–50 °C. 1H NMR: ($CDCl_3$, 400 MHz): δ (ppm): 8.44–8.46 (dd, $J = 1.7, 7.4$ Hz, 2H), 7.78–7.80 (d, $J = 7.1$ Hz), 7.51–7.56 (m, 2H), 7.06–7.09 (td, $J = 1.0, 7.3$ Hz, 2H). ^{13}C NMR: ($CDCl_3$, 400 MHz): δ (ppm): 154.4, 149.6, 137.5, 123.5, 121.2. MS (EI, 70 eV) m/z (relative intensity): 235 (42), 155 (7), 78 (98), 51 (100). Anal. calcd (%) for $C_{10}H_8N_2Se_2$: C, 51.07, H, 3.42, N, 8.01. Found: C, 51.12, H, 3.48, N, 7.97.

Crystallography

The single crystal X-ray data of **2e** was collected on a Bruker SMART Apex II CCD-based diffractometer at 180(2) K, using graphite monochromatized Mo-K α radiation ($\lambda = 0.71073$ Å). Data reduction was carried out using the SAINT-NT software package from Bruker AXS.²² The raw intensities were corrected for absorption effects through the multi-scan method with SADABS.²³ The structure was solved by a combination of direct methods and subsequent difference Fourier syntheses and refined by full matrix least squares on F^2 using the SHELX-2013 suite.²⁴ The hydrogen atoms were inserted at geometrical positions. Anisotropic thermal parameters were used for all non-hydrogen atoms, while the C–H hydrogen atoms were refined with isotropic parameters equivalent 1.2 times of the atoms to which they are attached. Molecular and crystal packing diagrams were drawn with Olex2 (ref. 25) and PyMOL, respectively.²⁶ The crystal data and refinement details of **2e** are summarized in the Table 4.

Anticarcinogenic activity

Anticarcinogenic activity of the synthesized compounds was evaluated against the Raji cancer cell line using the MTT colorimetric assay.²⁰ The stock solutions of the synthesized compounds were prepared by dissolving in the minimum volume of dimethyl sulfoxide (DMSO), which was further diluted to reach the appropriate volume. Cells (1×10^4 cells per well) were plated in 96-multiwell plates. After incubation for 48 h, MTT dissolved in phosphate buffer saline (PBS) was added to each well at a final concentration of 5 mg mL⁻¹ and then incubated at 37 °C and 5% CO₂ for 2 h. The Raji (acute lymphoid leukemia) cells were maintained in a humidified atmosphere of 5% CO₂, 95% air at 37 °C. Curcumin was used as a positive control and the wells containing DMSO (1%) and cell suspension was regarded as the negative control. The blank wells were consisted of 200 μ L of the RPMI medium. The microplates were

Table 4 Crystal data and relevant refinement details of **2e**

Empirical formula	$C_{12}H_{12}N_2Se$
M_w	263.20
Crystal system	Monoclinic
Space group	$P2_1/n$
$a/\text{\AA}$	7.5073(3)
$b/\text{\AA}$	19.2645(59)
$c/\text{\AA}$	7.5241(4)
$\beta/^\circ$	92.684(2)
$V/\text{\AA}^3$	1086.97(9)
Z	4
$D_c/\text{g cm}^{-3}$	1.608
μ/mm^{-1}	3.420
$F(000)$	528
2θ range/ $^\circ$	4.23–58.28
Index ranges	$10 \leq h \leq 9, 21 \leq k \leq 26, 10 \leq l \leq 10$
Reflections collected	17 964
Unique reflections, $[R_{\text{int}}]$	2930 [0.0501]
Goodness of fit on F^2	1.020
Final R indices	
$R_1, wR_2, [I > 2\sigma I]$	0.0306, 0.0583 [2287]
R_1, wR_2 (all data)	0.0481, 0.0640
Largest diff. peak/hole/ $e\text{\AA}^{-3}$	0.51/–0.44

further incubated for 48 h. To evaluate cell survival, each well was then incubated with 20 μ L of MTT solution (5 mg mL⁻¹ in PBS) and incubated for 4 h at 37 °C. The media in each well was replaced with 200 μ L DMSO and pipetted up and down to dissolve the formazan crystals which were formed by the cellular reduction of MTT. The absorbance of each well was measured at 570 nm using an ELISA reader. Each experiment was repeated three times. The results were expressed as the IC₅₀, which induces a 50% inhibition of cell growth of treated cells when compared to the growth of control cells.

Computational details

The entire quantum calculations were performed by using Gaussian 03 (ref. 27) program on a Pentium personal computer. Complete geometry optimizations were performed by density functional theoretical (DFT) computations by using the closed-shell Becke–Lee–Yang–Parr hybrid exchange–correlation three-parameter functional (B3LYP) in combination with 6-31 + G(d,p) basis set.²⁸

Conclusions

The discussed protocol affords analytically pure symmetrical monoselenide without any contamination of the respective diselenide. The reaction involves the formation of a selenated aluminato complex that undergoes pyridine-shift reaction leading to the generation of LiAlSeH₂ and symmetrical bis(2-pyridyl)selenide. The proposed mechanism has been validated by experimental observations, 1H NMR analysis and theoretical analysis. The theoretical analysis showed a strong tendency of the reaction between LiAlH₄ and bis(2-pyridyl) diselenides leading to the formation of complex (I). The synthesized compounds were also evaluated as

anticarcinogenic agents and compound **1f** showed anticarcinogenic activity comparable to the standard drug curcumin.

Acknowledgements

We are thankful to Mr Avtar Singh, CIL, Punjab University, Chandigarh, for NMR spectra.

Notes and references

- 1 D. M. Freudendahl, S. A. Shahzad and T. Wirth, *Eur. J. Org. Chem.*, 2009, **42**, 1649.
- 2 (a) J. Wang, P. Liu, C. C. Seaton and K. M. Ryan, *J. Am. Chem. Soc.*, 2014, **136**, 7954; (b) J. Gu, Z.-Q. Zhao, Y. Ding, H.-L. Chen, Y.-W. Zhang and C.-H. Yan, *J. Am. Chem. Soc.*, 2013, **135**, 8363.
- 3 (a) A. Molter, G. N. Kaluđerović, H. Kommera, R. Paschke, T. Langer, R. Pöttgen and F. Mohr, *J. Organomet. Chem.*, 2012, **701**, 80; (b) Y. A. Lin, O. Boutureira, L. Lercher, B. Bhushan, R. S. Paton and B. G. Davis, *J. Am. Chem. Soc.*, 2013, **135**, 12156; (c) M. R. Nicole, N. M. R. McNeil, M. C. Matz and T. G. Back, *J. Org. Chem.*, 2013, **78**, 10369; (d) F. Martínez-Ramos, H. Salgado-Zamora, M. E. Campos-Aldrete, E. Melendez-Camargo, Y. Márquez-Flores and M. Soriano-García, *Eur. J. Med. Chem.*, 2008, **43**, 1432; (e) P. Arsenyan, K. Rubina, I. Shestakova and I. Domracheva, *Eur. J. Med. Chem.*, 2007, **42**, 635; (f) J. S. Dhau, A. Singh, A. Singh and B. S. Sooch, *Phosphorus, Sulfur Silicon Relat. Elem.*, 2014, **189**, 687.
- 4 (a) K. Shimada, S. Oikawa, H. Nakamura, K. Moro-oka, M. Kikuchi, A. Maruyama, T. Suzuki, H. Kogawa, Y. Inoue, Y. Gong, S. Aoyagi and Y. Takikawa, *Bull. Chem. Soc. Jpn.*, 2005, **78**, 899; (b) K. K. Bhasin, V. K. Jain, H. Kumar, S. Sharma, S. K. Mehta and J. Singh, *Synth. Commun.*, 2003, **33**, 977; (c) A. S. Hodage, P. C. Parashiva, P. P. Phadnis, A. Wadawale, K. I. Priyadarsini and V. K. Jain, *J. Organomet. Chem.*, 2012, **720**, 19; (d) F. M. Libero, M. C. D. Xavier, F. N. Victoria, P. S. Nascente, L. Savegnago, G. Perin and G. Alves, *Tetrahedron Lett.*, 2012, **53**, 3091; (e) A. L. Braga, W. A. S. Filho, R. S. Schwab, O. E. D. Rodrigues, L. Dornelles, H. C. Braga and D. S. Lüdtke, *Tetrahedron Lett.*, 2009, **50**, 3005; (f) R. K. Sharma, G. Kedarnath, A. Wadawale, C. A. Betty, B. Vishwanadh and V. K. Jain, *Dalton Trans.*, 2012, **41**, 12129; (g) R. K. Sharma, G. Kedarnath, V. K. Jain, A. Wadawale, C. G. S. Pillai, M. Nalliath and B. Vishwanadh, *Dalton Trans.*, 2011, **40**, 9194.
- 5 (a) K. K. Bhasin and J. Singh, *J. Organomet. Chem.*, 2002, **658**, 71; (b) E. N. Deryagina, N. V. Russavskaya, L. K. Papernaya, E. P. Levanova, E. N. Sukhomazova and N. A. Korchevin, *Russ. Chem. Bull.*, 2005, **54**, 2473.
- 6 (a) J. S. Dhau, A. Singh, Y. Kasetti and P. V. Bharatam, *Eur. J. Org. Chem.*, 2012, 1746; (b) J. S. Dhau, A. Singh, Y. Kasetti, S. Bhatia, P. V. Bharatam, P. Brandão, V. Félix and K. N. Singh, *Tetrahedron*, 2013, **69**, 10284; (c) J. S. Dhau, A. Singh and R. Dhir, *J. Organomet. Chem.*, 2011, **696**, 2008.
- 7 S. Kumar, H. Johansson, L. Engman, L. Valgimigli, R. Amorati, M. G. Fumo and G. F. Pedulli, *J. Org. Chem.*, 2007, **72**, 2583.
- 8 J.-M. Becht and C. L. Drian, *J. Org. Chem.*, 2011, **76**, 6327.
- 9 N. Mukherjee, T. Chatterjee, C. Brindaban and B. C. Ranu, *J. Org. Chem.*, 2013, **78**, 11110.
- 10 V. P. Reddy, A. V. Kumar and K. R. Rao, *J. Org. Chem.*, 2010, **75**, 8720.
- 11 H. Ishihara, M. Koketsu, Y. Fukuta and F. Nada, *J. Am. Chem. Soc.*, 2001, **123**, 8408.
- 12 (a) J. S. Dhau, A. Singh, A. Singh, B. S. Sooch, P. Brandão and V. Félix, *Inorg. Chim. Acta*, 2012, **392**, 335; (b) J. S. Dhau, R. Dhir and A. Singh, *J. Organomet. Chem.*, 2011, **696**, 2406.
- 13 G. Zhao, H. Lin, S. Zhu, H. Sun and Y. Chen, *Anti-Cancer Drug Des.*, 1998, **13**, 767.
- 14 K. K. Bhasin, Rishu, S. Singh, H. Kumar and S. K. Mehta, *J. Organomet. Chem.*, 2010, **695**, 648.
- 15 (a) J. S. Dhau, R. Dhir, A. Singh, A. Singh, P. Brandão and V. Félix, *Tetrahedron*, 2014, **70**, 4876; (b) A. Singh, J. S. Dhau, N. Sharma and A. Singh, *Inorg. Chim. Acta*, 2015, **432**, 109; (c) J. S. Dhau, A. Singh, A. Singh, B. S. Sooch, P. Brandão and V. Félix, *J. Organomet. Chem.*, 2014, **766**, 57.
- 16 J. A. Gladysz, J. L. Hornby and J. E. Garbe, *J. Org. Chem.*, 1978, **43**, 1204.
- 17 N. Sklar and B. Post, *Inorg. Chem.*, 1967, **6**, 699.
- 18 (a) H. G. Mautner, S.-H. Chu and C. M. Lee, *J. Org. Chem.*, 1962, **27**, 3671; (b) A. Toshimitsu, S. Owada, S. Uemura and M. Okano, *Tetrahedron Lett.*, 1980, **21**, 5037; (c) K. Smith, I. Matthews, N. M. Hulme and G. E. Martin, *J. Chem. Soc., Perkin Trans. 1*, 1986, 2075; (d) Y. Cheng, J. Emge and J. G. Brennan, *Inorg. Chem.*, 1994, **33**, 3711.
- 19 S. J. Dunne, E. I. von Nagy-Felsobuki and M. F. Mackay, *Acta Crystallogr., Sect. C: Cryst. Struct. Commun.*, 1995, **51**, 1454.
- 20 A. Monks, D. Scudiero, P. Skehan, R. Shoemaker, K. Paull, D. Vistica, C. Hose, J. Langley and P. Cronise, *J. Natl. Cancer Inst.*, 1991, **83**, 757.
- 21 C. O. Kienitz, C. Thöne and P. G. Jones, *Inorg. Chem.*, 1996, **35**, 3990.
- 22 Bruker SAINT-plus, Bruker AXS Inc., Madison, Wisconsin, USA, 2007.
- 23 G. M. Sheldrick, *SADABS*, University of Göttingen, Germany, 1996.
- 24 G. M. Sheldrick, *Acta Crystallogr., Sect. A: Found. Crystallogr.*, 2008, **64**, 112.
- 25 O. V. Dolomanov, L. J. Bourhis, R. J. Gildea, J. A. K. Howard and H. Puschmann, OLEX2: a complete structure solution, refinement and analysis program, *J. Appl. Crystallogr.*, 2009, **42**, 339.
- 26 PyMOL Molecular Graphics System, Version 1.2r2, DeLano Scientific LLC, 2009.
- 27 M. J. Frisch, et al., *GAUSSIAN 03 Program*, Gaussian, Inc., Wallingford, CT, 2004.
- 28 P. Perdew and Y. Wang, *Phys. Rev. B: Condens. Matter Mater. Phys.*, 1992, **45**, 13244.